

Resistivity and Hall Effect of Germanium at Low Temperatures*

C. S. HUNG† AND J. R. GLIESSMAN‡
 Department of Physics, Purdue University, Lafayette, Indiana
 (Received July 21, 1954)

An experimental investigation of the Hall effect and the resistivity of germanium alloys at temperatures from room temperature down to the liquid helium temperature range is reported. Germanium samples with different kinds of impurity and different concentrations were used. At higher temperatures, satisfactory agreement between theory and experiment was found. The activation energy of the impurity states was found to be of the order of 10 millivolts. The scattering of the carriers in the conduction and filled bands consists mainly of lattice scattering and ionized impurity scattering. At low temperatures, however, anomalies in the Hall curves were observed. The Hall curve for every sample measured went through a maximum as the temperature was lowered. At the same time the resistivity approached a saturation value. The Hall curves of low resistivity samples finally became flat at very low temperatures. These anomalies are explained on the assumption of small but finite mobility of carriers in the impurity states. This conduction in the impurity states assumes importance at low temperatures when the concentration of carriers in the conduction band becomes very low. When this simultaneous conduction in the conduction band and the impurity band is considered, the behaviors in the Hall and the resistivity curves are satisfactorily explained. The mobility in the impurity band is found to increase with the impurity concentration, but is rather temperature-independent.

I. INTRODUCTION

A. Object of This Work

PREVIOUS measurements¹ of the Hall effect and the resistivity of germanium at temperatures between 80°K and 900°K have shown that germanium behaves as an impurity semiconductor. The concentration of electrons in the conduction band and of holes in the filled band follow the dissociation equation as predicted by theory.² The scattering of the electrons and the holes is due mainly to lattice vibrations and to Coulomb scattering by the ionized impurity centers.³

The flatness of the Hall coefficient *versus* temperature curves for temperatures between 300°K and 80°K indicates that the activation energies of the impurity states in germanium are very low. Furthermore, for some samples, the concentration of electrons in the conduction band (or the concentration of holes in the filled band) is so large that the assembly of electrons must be treated as a degenerate gas in this temperature range.⁴

It would be interesting, therefore, to investigate the behavior of germanium at lower temperatures in order to determine the activation energies of the impurity states, the behavior of the degenerate electron gas at very low temperatures, and to check the theory of scat-

tering at low temperatures. Samples prepared and selected at Purdue University have been investigated by Ambrose,⁵ who measured the resistivity down to liquid helium temperatures, and by Estermann and co-workers,⁶ who investigated resistivity and Hall effect down to the liquid hydrogen temperature range. Anomalies observed at low temperatures, especially by the latter group, prompted the undertaking of the current program of low-temperature investigation at Purdue University.

This paper reports the measurements of resistivity and Hall effect from room temperature down to liquid helium temperatures, the extent of agreement with theory based on the usual model of impurity semiconductor, the anomalies observed at low temperatures, and the modification of the model proposed in order to explain the anomalies.

B. Germanium as an Impurity Semiconductor

Figure 1 illustrates the simple energy level diagram for germanium as an impurity semiconductor. N_D and N_A are the concentrations of donors and acceptors, respectively. ΔE_D and ΔE_A are the respective energy gaps from the conduction and filled bands. These energy

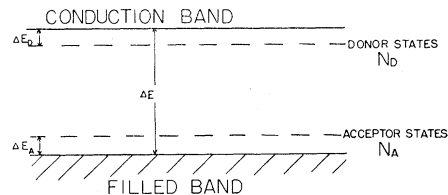


FIG. 1. Energy-level diagram for an impurity semiconductor.

* Work supported by the U. S. Army Signal Corps contracts with Purdue University.

† Last known address: University of Leiden, Leiden, The Netherlands.

‡ Now at Hughes Aircraft Company, Culver City, California.

¹ Lark-Horovitz, Middleton, Miller, and Walerstein, *Phys. Rev.* **69**, 258 (1946); A. E. Middleton and W. W. Scanlon, *Phys. Rev.* **92**, 219 (1953), especially Figs. 6, 7, and 9.

² R. H. Fowler, *Proc. Roy. Soc. (London)* **A140**, 505 (1933).

³ K. Lark-Horovitz and V. A. Johnson, *Phys. Rev.* **69**, 258 (1946); K. Lark-Horovitz, *Elec. Eng.* **68**, 1047 (1949); H. C. Torrey and C. A. Whitmer, *Crystal Rectifiers* (McGraw-Hill Book Company, Inc., New York, 1948), pp. 58-61.

⁴ V. A. Johnson and K. Lark-Horovitz, *Phys. Rev.* **71**, 374, 909 (1947); **72**, 531 (1947).

⁵ J. R. Ambrose, Naval Research Laboratory (private communication).

⁶ I. Estermann and A. Foner, *Phys. Rev.* **79**, 365 (1950); I. Estermann, Carnegie Institute of Technology ONR reports (unpublished).

gaps, for germanium, are usually small compared to the energy gap between the filled band and the conduction band. ΔE_D and ΔE_A are of the order of 0.01 ev as measured at low temperature, whereas ΔE is about 0.75 ev.

The measurements to be discussed were made at temperatures low enough for the contribution of intrinsic electrons and holes to be neglected. The impurity states are usually considered as localized states such that there is no conduction in them. Carriers of only one sign are present. If $N_D > N_A$, the carriers will be electrons in the conduction band, and the sample is *N*-type. Conversely, if $N_A > N_D$, the carriers will be holes in the filled band, and the sample is *P*-type. Only *N*-type samples will be discussed, but the same considerations may be readily extended to *P*-type samples.

When there is only one kind of carrier, the Hall coefficient is given by

$$R = \pm r/ne, \quad (1)$$

where n is the concentration of free carriers. The sign of the Hall coefficient coincides with the sign of the charge carriers; r is a numerical factor of the order of unity and is dependent on the statistics obeyed by the carriers and on the nature of the collisions between the carriers and the lattice and impurity ions.⁷

With a small but finite energy gap between the donor states and the conduction band, the concentration of electrons is expected to decrease rapidly with decreasing temperature, as soon as kT becomes smaller than ΔE_D . The Hall coefficient R is then expected to increase rapidly with decreasing temperature.

The resistivity is given by

$$\rho = (ne\mu)^{-1} \quad (2)$$

where

$$1/\mu = 1/\mu_L + 1/\mu_I; \quad (3)$$

μ is the mobility of the electrons in the conduction band. $1/\mu_L$ and $1/\mu_I$ correspond to the scattering of the electrons due to lattice vibrations and by the impurity ions, respectively. Furthermore,

$$\mu_L = A(T/300)^{\frac{3}{2}}, \quad (4)$$

where A corresponds to the value of μ_L at room temperature and is of the order of 3600 cm²/volt-sec when T is expressed in °K. The scattering by the impurity ions is of the nature of Coulomb scattering, and the expression given by Conwell and Weisskopf,⁸ is

$$\mu_I = \frac{8.25 \times 10^{17} T^{\frac{3}{2}}}{N_s \ln\{1 + 2.57 \times 10^8 (N_s)^{-\frac{2}{3}} T^2\}} \text{ cm}^2/\text{volt-sec}, \quad (5)$$

where N_s is the concentration of Coulomb scattering centers. The above analysis has been found satisfactory

⁷ V. A. Johnson and K. Lark-Horovitz, Phys. Rev. **82**, 977 (1951); H. Jones, Phys. Rev. **81**, 149 (1951).

⁸ E. Conwell and V. F. Weisskopf, Phys. Rev. **69**, 258 (1946); **77**, 388 (1950).

above liquid air temperature when N_s is assumed equal to the carrier density n . Previously this analysis was found to be satisfactory when applied for the resistivities measured down to liquid air temperatures using the relation $N_s = n$. During the course of this work, it was found that, for samples of high resistivity, the above analysis is satisfactory⁹ down to 10°K, provided that the concentration of scattering centers is taken as $N_s = n + 2N_A$.

Since μ_I is a slowly varying function of the temperatures, while n varies exponentially with T , the resistivity is expected to increase indefinitely as the temperature is lowered.

In Sec. III it will be shown that, at very low temperatures, the resistivity and Hall coefficient do not increase indefinitely with $1/T$ according to the picture above. Instead, as the temperature is lowered, the Hall coefficient is found to pass through a maximum. At the same time, the resistivity is found to approach saturation. This leads to the conclusion discussed in Sec. IV that the conduction in the impurity states must be taken into consideration, especially at very low temperatures.

II. EXPERIMENTAL PROCEDURE

A. Preparation of Samples

The samples used were obtained from W. E. Taylor, formerly of the Physics Department of Purdue University. The antimony-doped samples were obtained by adding antimony to high purity germanium so that there was only one predominant impurity in these samples. The neutron-bombarded samples were originally high-resistance *N*-type. Slow neutrons cause transmutations of the germanium atoms resulting in the introduction of both gallium and arsenic impurities.¹⁰ The samples were annealed to heal the displacements caused by the fast neutrons. It was calculated that the ratio of gallium atoms to arsenic atoms was about 3 to 1. Gallium is a *P*-type and arsenic is an *N*-type impurity. In such a case, there would be four impurity scattering centers produced but only two *P*-type carriers due to the recombination of one electron with one hole.

The samples are cut from an ingot to a size of about 1 cm × 2 mm × 5 mm. The samples are then ground with No. 600 carborundum and etched to reduce surface effects. The etching solution contains hydrofluoric acid and cupric nitrate.¹ It could be seen after etching that the samples were mostly single crystals. Some samples were ground again and used without additional etching. Preliminary measurements of the room temperature resistivities along the length of the sample showed the samples to be homogeneous. It was found later, however, that, in some cases, inhomogeneities appeared at low temperatures.

The current and potential leads are 0.002-in. enamel-

⁹ C. S. Hung and V. A. Johnson, Phys. Rev. **79**, 535 (1950).

¹⁰ Cleland, Lark-Horovitz, and Pigg, Phys. Rev. **78**, 814 (1950).

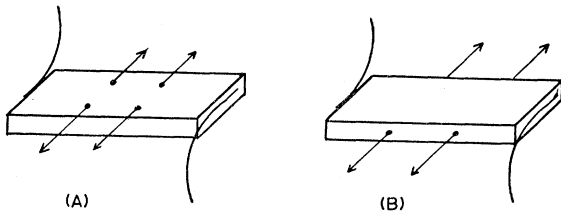


FIG. 2. Two types of current lead and probe arrangement which were used.

covered copper wires that are attached to the sample with Cerroseal 35 solder. This solder consists mostly of tin with a small quantity of indium. It is very malleable at room temperatures and assures good contact at low temperatures. The sample is first cleaned with alcohol and then the solder put on the ends and on four spots in the middle, using zinc chloride flux. The size of the solder spots for the potential leads are kept as small as possible to minimize shorting the sample with solder. The size of these spots is of the order of 0.2 to 0.4 mm in diameter. The four potential leads and the two current leads are arranged as shown in Fig. 2. This probe arrangement permits two Hall measurements and two resistivity measurements simultaneously. The advantage of this is that one can detect inhomogeneities that may become pronounced at low temperatures. Furthermore, the measurement can be continued even if a poor contact develops at one of the soldered probes.

There is some uncertainty about the two points

between which the probe separation should be measured. If the probe distances are measured to be about 0.1 to 0.2 cm, there is the possibility of an error of about 20 percent to 30 percent. This error will appear in the absolute value of the Hall coefficient and the resistivity. It is possible to reduce this error in the case of the Hall probes by soldering the probes to the side of the sample as shown in Fig. 2(B). Then the width of the sample, which is rather easily measured, is equivalent to the distance between the Hall probes.

It is desirable to check the effect that soldered contacts might have on the measurements at low temperatures. For this reason measurements were repeated on one of the samples with pressure contacts. The four spots shown in Fig. 2 were plated with rhodium, and then the probes were pressed onto the plated spots.

All of the samples are placed on holders made of Bakelite or baked lavite and then put into the cryostat.

B. The Cryostat

The cryostat was constructed so that a continuous range of temperatures from 1.3°K to 300°K could be obtained. The cryostat proper and the devices for the control and calibration of temperature are shown in Fig. 3.

The sample is enclosed in the copper cylinder (A), which forms the bulb of a gas thermometer. This, in turn, is enclosed in a brass cylinder (B). The space

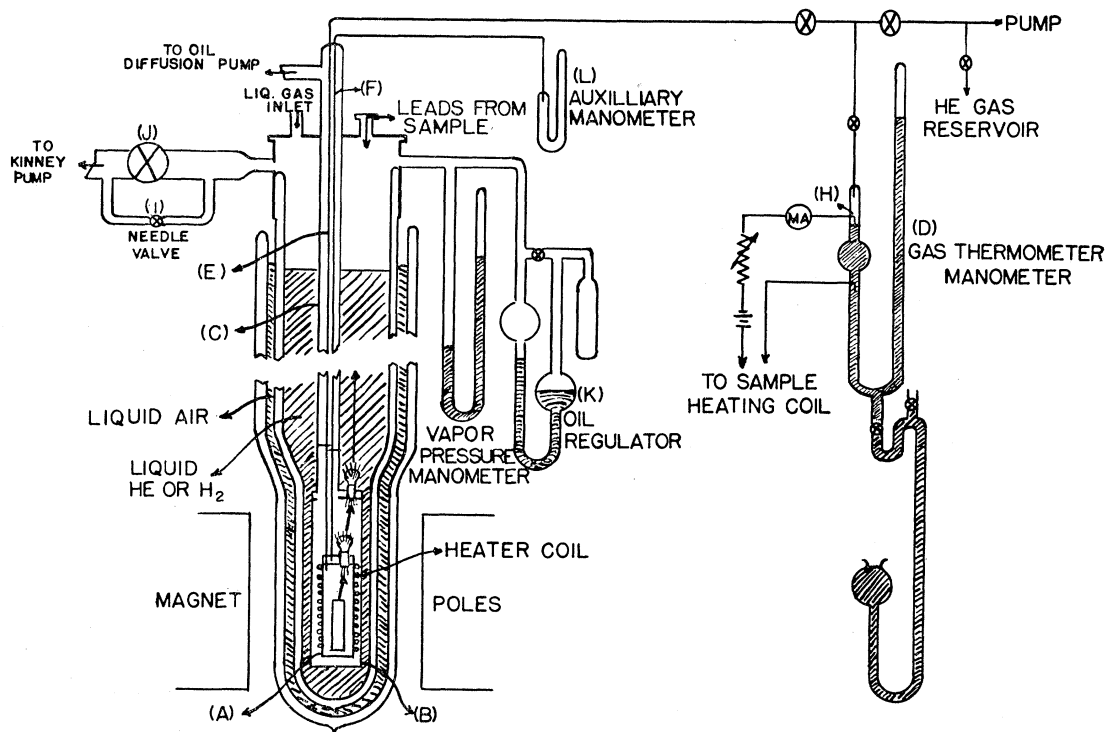


FIG. 3. The cryostat and devices for the control and calibration of temperature.

between the cylinders is part of a high vacuum system that is connected to an oil diffusion pump through the monel tubing (C). It can be pumped to a vacuum of better than 10^{-5} mm Hg pressure. The space between the two cylinders serves to insulate the gas thermometer bulb from the liquid bath. A heater wire is wound non-magnetically around the gas thermometer bulb and is used to heat the sample to temperatures above that of the liquid bath.

The gas thermometer bulb is connected to a mercury manometer (D) outside through a capillary (E) with an inside diameter of 1 mm. An auxiliary capillary (F) is placed alongside the gas thermometer capillary (E) and in thermal contact with it. The auxiliary capillary is used in conjunction with a small closed-end manometer (L) and serves as a method of correcting for the temperature gradient that exists along the capillary in the calculation of temperature. These two capillaries are then run up through the monel tubing (C). They are thermally insulated from the liquid bath except near the lower end so that the average temperature of the capillaries is in the order of 50°K , when a liquid helium bath is used. The capillary correction to the temperature calibration is, therefore, small. The temperature calibration is accurate to within 1 percent.

There is no direct heat leak to the inside of the gas thermometer bulb from room temperature. The bulb is entirely shielded by the brass cylinder (B) and the high-vacuum pumping line (C). The leads to the sample enter through two offset copper to glass seals. The monel tubing (C) is provided with a light shield (G). The heat leak from the gas thermometer bulb to the bath comes from the capillary tubings, and from the sample leads.

It is possible to control automatically the temperature above that of the liquid bath with a simple device which is built into the manometer (D). The level of the mercury, in conjunction with a tungsten wire (H), serves as a heater current switch. As the level of the mercury rises or falls with a change in temperature, contact is made or broken with the tungsten wire, turning the heater current on or off, as the case may be. The variation in pressure of the mercury is less than 0.4 percent.

Temperatures below those of the liquified gases are obtained by reducing the vapor pressure of the bath. Thermal contact between the sample and the bath is established by introducing exchange helium gas into the vacuum space. A needle valve (I) by-passing the 2-in. diameter packless valve (J) is used for controlling the pumping speed. The vapor pressure is maintained constant with the aid of an oil regulator (K).

The leads from the sample are placed around the monel tubing (C) and are relatively susceptible to stray electric fields. For this reason, it is desirable to provide shielding for the leads when high-resistance samples are to be measured. This has been done in a second cryostat by running the wires down to the sample through the

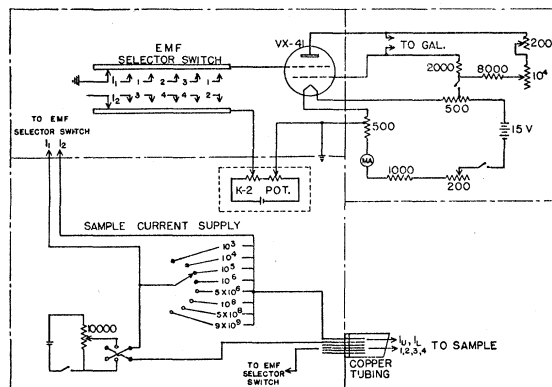


FIG. 4. Electrometer circuit used when sample resistance exceeds 10^6 ohms.

monel tubing (C). They are separated by polystyrene spacers to minimize the capacity between the wires.

C. The Electrical Measuring Circuit

(a) *Potentiometer and Galvanometer Circuit for Use with Low Resistance Samples*

The potential developed across the sample probes is balanced against a Leeds and Northrup type K-2 potentiometer to obtain a null reading on a reflecting galvanometer. Heavy copper knife switches are used in the emf selector switches and the emf reversing switch to minimize contact potential. The sample current source is a 6-volt storage battery connected through a series of variable resistances. The current is measured by measuring the potential drop across a standard 10-ohm resistor with the potentiometer.

The galvanometer used is Leeds and Northrup type 2500B with a current sensitivity of 3×10^{-10} amp/mm and an external damping resistance of 10 000 ohms. The period of the galvanometer is 7 seconds. The voltage sensitivity of the circuit is 3 microvolts/mm. For very low-resistance samples, a low-resistance galvanometer is used to obtain better voltage sensitivity.

(b) *Electrometer Tube Circuit for Use with High-Resistance Samples*

When the resistance of the samples is higher than 10^4 ohms, the voltage sensitivity of the galvanometer decreases with increasing resistance. For high-resistance samples at low temperatures, an electrometer circuit (Fig. 4) is used. This circuit employs a VX-41 Victoreen electrometer tube with the Leeds and Northrup 2500B galvanometer in the output. The potential to be measured is applied to the control grid and balanced with the potentiometer. Upon measuring, a balance is indicated by a zero deflection of the galvanometer when the control grid ground switch is opened.

The emf selector switch has polystyrene insulation to minimize electrical leakage and gold contacts for low contact resistance. The electrometer is generally used

TABLE I. List of germanium samples investigated.

Specification	Sample No.	Type	Room temperature resistivity (ohm-cm)
High purity	HP-1	<i>N</i>	15
High purity	HP-2	<i>P</i>	7.5
Sb added	SB-2	<i>N</i>	0.4
Sb added	SB-1	<i>N</i>	0.3
Sb added	SB-3	<i>N</i>	0.1
Sb added	SB-4	<i>N</i>	0.04
Sb added	SB-5	<i>N</i>	0.004
Neutron-bombarded	B-1	<i>P</i>	0.6
Neutron-bombarded	B-2	<i>P</i>	0.2
Neutron-bombarded	B-3	<i>P</i>	0.05

when the sample resistance is greater than 10^5 ohms. The useful sensitivity of the electrometer circuit is 150 microvolts/mm. For sample resistance of less than 10^{10} ohms it is not necessary to take into account the control grid current for emf correction. This control grid current is about 10^{-14} amp.

The leads from the cryostat are brought to the electrometer circuit unit through copper tubing for shielding purposes and are spaced with polystyrene insulators to minimize capacitance to ground.

The sample current is again determined from the potential drop across a standard resistor. A selection of resistors varying from 10^3 to 9×10^9 ohms is available.

It is possible to switch the galvanometer from the plate circuit to the grid circuit of the electrometer tube. Then one can utilize the sample current source of the electrometer unit and the aforementioned shielding without using the electrometer tube itself.

D. The Magnet

The magnetic field from an electromagnet with pole faces four inches in diameter and a variable pole gap is used. The magnet is calibrated with a GE fluxmeter. With a pole gap of 5 cm, a field of 5000 gauss is obtained with a current of 15 amp.

The disturbances of the magnetic field by the glass Dewars, the liquified gas and the brass and copper cylinders, (a) and (b) of Fig. 3, are negligible at all temperatures. The tin solder is not superconducting at any temperature with a magnetic field above 300 gauss.¹¹ The Wood's metal solder is not expected to be superconducting at a magnetic field much above 1000 gauss.

III. EXPERIMENTAL RESULTS

Measurements were made on the samples listed in Table I. For each measurement of Hall emf or resistivity, four readings are taken with opposite directions of sample current and opposite directions of magnetic field to eliminate thermal emf and pickup in the circuit. Most of the measurements were made with soldered current and potential leads. For sample SB-1, measure-

ments were made with both ground and etched surfaces, and the results were essentially the same, both on the Hall measurements and the resistivity measurements, at all temperatures. Measurements were also made on sample SB-2, both with soldered leads and with pressure contacts, and the results were the same.

It was found that measurements on the same sample in different runs may differ by a few percent, but the shapes of the Hall and the resistivity *vs* temperature curves were the same.

A sample homogeneous at room temperature may show very large inhomogeneity at very low temperatures. The values of resistivities from the two sets of probes may then differ by a factor of 2 or 3 even though the sample is quite uniform in the liquid hydrogen temperature range. Measurements on the same sample with the potential leads resoldered to apparently the same positions may therefore yield different values at very low temperatures. However, the shapes of the Hall and the resistivity curves again remain the same. No essential difference was found between measurements made with increasing temperature and with decreasing temperature.

The magnetic fields used in the Hall measurements were usually between 1 and 5 kilogauss. The larger field was used when the Hall emf is small. The magnetic field dependence of the Hall coefficient was checked for every sample for at least a few points spaced evenly on the $1/T$ curve. In some cases the Hall coefficient and the resistivity for a magnetic field of 5 kilogauss may be higher by 30 percent than the values at 1 kilogauss, but this effect of magnetic field dependence does not change the essential characteristics of the Hall coefficient and resistivity *versus* temperature curves.

The measurements were also made with different currents through the sample. The electric field in the sample was usually from 10 millivolt per cm to 1 volt per cm, except for the extremely low resistance samples for which the field might be below 1 millivolt per cm. The current was limited in the case of low-resistance samples by the consideration of heat input to the sample. The values of Hall coefficient and resistivity were essentially independent of the current for fields between a few millivolts/cm and a few hundred millivolts/cm.

A. The Hall Measurements

The High-Purity and the Antimony-Doped Samples

In Fig. 5 are shown the Hall coefficient *versus* $1/T$ curves for the high-purity and the antimony-doped samples. For the higher resistivity samples, including HP-1, HP-2, SB-1, SB-2, and SB-3, the curves can be conveniently divided into three sections: (a) the exhaustion range, where the Hall coefficient is almost constant, (b) the intermediate-temperature range where the Hall coefficient increases rapidly with decreasing temperature, and (c) the low-temperature

¹¹ J. G. Daunt and K. Mendelssohn, Proc. Roy. Soc. (London) **A160**, 127 (1937).

range where the Hall coefficient vs $1/T$ curve goes through a maximum and drops rapidly with decreasing temperature. For low-resistivity samples, this division is not easily made. For the first two temperature regions, the model presented in Sec. I serves as a satisfactory basis for discussion.

(a) *The exhaustion range.*—Within this range, all the electrons from the donor states are excited into the conduction band and so the concentration of carriers is constant with temperature. Equation (1) then indicates that the Hall coefficient would be constant except for the temperature dependence of r .⁷ In Fig. 6 is shown an enlargement of the Hall coefficient graph in the exhaustion ranges of the various samples. The upper temperature limit of the exhaustion range for most samples extends to room temperature, except for the highest resistivity sample HP-1 for which the intrinsic contribution of carriers becomes appreciable above 200°K. The lower temperature limit of the exhaustion range extends to temperatures near 30° or 40°K for the higher resistivity samples. This is to be expected from their low activation energy. It is to be noticed in Fig. 6 that the slope of the Hall coefficient vs $1/T$ curve, as the temperature is lowered from room temperature, is lower for samples of higher purity. Finally, for the highest resistivity samples, the Hall coefficient actually goes down as T is lowered from room temperature, and reaches a minimum at about 80°K. This behavior of the Hall coefficient, especially the minimum in the curve, suggests that in this region the dependence⁷ of r on T is predominant over the dependence of n on T , since one does not expect the concentration of carriers to increase as the temperature is lowered.

(b) *The intermediate-temperature range.*—In this range

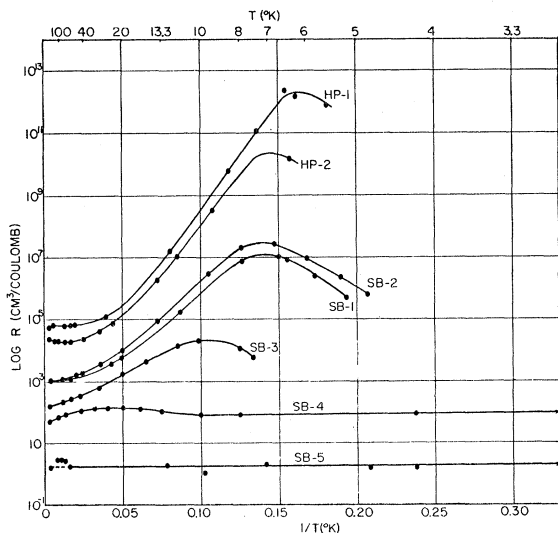


FIG. 5. Semilogarithmic plot of the Hall coefficient vs reciprocal of Kelvin temperature for high-purity undoped germanium samples HP-1 and HP-2 and antimony-doped germanium samples SB-1, SB-2, SB-3, SB-4, and SB-5. All these samples are N -type except HP-2.

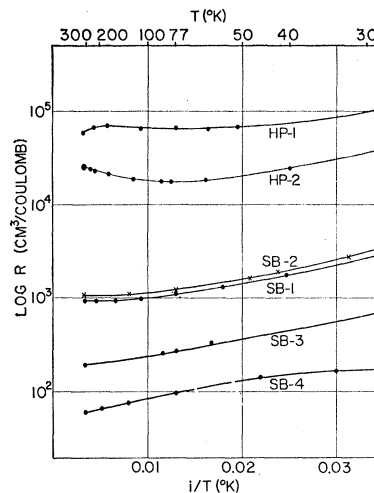


FIG. 6. Enlargement of a section of Fig. 5 to show details of Hall effect behavior in the exhaustion range.

the Hall coefficient rises rapidly with decreasing temperature. The dependence of n on T is now predominant. The linear logarithmic increase of R , or the linear logarithmic decrease of n with $1/T$, is expected from the simple model with a rather sharp impurity level. The activation energy obtained from the slope of the $\log R vs 1/T$ curves by use of the dissociation equation² are shown in Table II.

(c) *The low-temperature range.*—For all samples measured, the Hall coefficients do not increase indefinitely as the temperature is lowered; instead the Hall coefficient goes through a maximum and then drops rapidly as T is lowered. The temperature at which this maximum occurs is higher for samples of higher impurity content. At temperatures below the maximum, the Hall coefficients of the higher-resistivity samples continue to drop as long as the Hall values remain measurable. On the basis of comparison with the neutron-bombarded samples (Fig. 7), one might expect all Hall curves to level out to constant values at temperatures well below the maximum.

It is important to note here that the values of the Hall coefficient in the neighborhood of the maximum of the Hall curve are practically independent of the magnetic field for fields between 1000 and 5000 gauss and also independent of the current through the sample for currents varying by a factor of ten.

It is improbable that the concentration of electrons in the conduction band should increase with decreasing temperature. Furthermore, r cannot be expected to change by more than a factor of 2, according to the free electron theory.

Nonuniformity in the impurity concentration of the sample, either macroscopic or microscopic, can cause a decrease in the Hall coefficient, even though the carrier density remains constant or decreases with decreasing temperature. However, accounting for the large drop

TABLE II. Sample properties.

Sample	n_0 , carrier density in exhaustion range (cm^{-3})	N_0 , scattering center density at 0°K (cm^{-3})	$N_D = n_0 + \frac{1}{2}N_0$ (or N_A for P-type) (cm^{-3})	Activation energy (ev)	Saturation resistivity at low temperatures (ohm-cm)	Donor (or acceptor) band mobility ($\text{cm}^2/\text{volt-sec}$)
HP-1 (N)	1.2×10^{14}	10^{14}	1.7×10^{14}	0.0135	4×10^8	1.5×10^{-4}
HP-2 (P)	2.5×10^{14}	10^{15}	7.5×10^{14}	0.0123	10^7	3×10^{-3}
SB-1 (N)	7.0×10^{15}	1.8×10^{15}	7.9×10^{15}	0.0093	2×10^4	0.05
SB-2 (N)	7.0×10^{15}	2×10^{15}	8.0×10^{15}	0.0083	10^5	0.01
SB-3 (N)	4.5×10^{16}		4.5×10^{16}	0.0055	3×10^2	0.5
SB-4 (N)	1.5×10^{17}		1.5×10^{17}		0.5	100
SB-5 (N)	4.0×10^{18}		4.0×10^{18}		0.0045	
B-1 (P)	8.5×10^{15}	8.5×10^{15}	1.3×10^{15}	0.0090	3×10^2	2.8
B-2 (P)	3.3×10^{16}	3.3×10^{16}	5×10^{16}		3	67
B-3 (P)	1.8×10^{17}	1.8×10^{17}	2.7×10^{17}		0.1	400

in the Hall coefficient observed below the maximum in some samples requires too artificial an arrangement of the impurity centers. Besides, it does not explain the systematic shifting of the Hall curve maxima to higher temperatures as the impurity content goes up. The sharp decrease of the Hall coefficient therefore must mean a breakdown of the simple model presented in Sec. I. Among the factors affecting this breakdown of Eq. (1) are the total concentration of impurity ions (N_D for N -type Ge) and the concentration of carriers at the temperature where this occurs.

For the lowest resistivity samples, SB-4 and SB-5, the division into these three regions seems rather artificial. It is hard to say from the Hall curves alone whether the intermediate-temperature range and the low-temperature range are absent or whether they have merged into one with the exhaustion range. Comparison with the resistivity curves, as discussed in the next section, however, gives more information about the nature of these Hall curves.

For the present, it will be noted that the activation energy for sample SB-4 is certainly not equal to zero, despite the flatness of the Hall curve. For sample SB-5, whether the activation energy is zero or not is immaterial to the conduction.

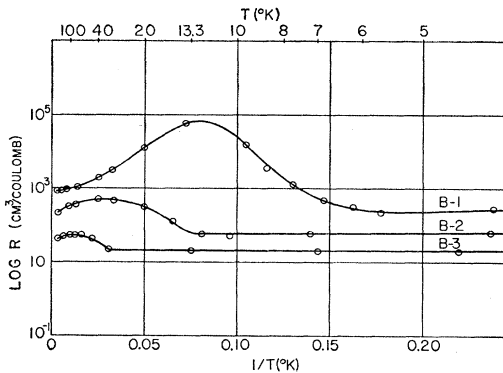


FIG. 7. Semilogarithmic plot of the Hall coefficient *vs* reciprocal of Kelvin temperature for germanium samples, initially N -type, but converted to P -type by neutron bombardment.

The Bombarded Samples

In Fig. 7 are shown the Hall curves for the neutron-bombarded samples. The same division into the three temperature regions applies. In the case of the highest-resistivity sample, B-1, this division is easily made, and the activation energy is found to be approximately 0.009 ev. For the two lower-resistivity samples, the intermediate-temperature regions are rather short, and the values of their activation energies cannot be readily ascertained.

The concentration of carriers in sample B-1 at its Hall maximum is less than the carrier concentrations in antimony-doped samples SB-1, SB-2, and SB-3 at the same temperature, and the Hall coefficients and resistivities of these latter samples are still rising rapidly at this temperature. This fact implies that the low-temperature behavior depends not only on the carrier concentration at a given temperature but also on the concentration of impurity centers (N_D for N -type). As mentioned in Sec. I, the impurity concentration of a bombarded sample is apt to be much higher than that of an antimony-doped sample having the same number of carriers at room temperature.

For the other two bombarded samples, the maxima in the Hall curves appear at still higher temperatures. The shifting of the maximum in the Hall curve to higher temperature as the impurity concentration of the sample becomes higher is similar to that observed for the pure and the antimony-doped samples.

B. The Resistivity Measurements

The resistivity *versus* $1/T$ curves for the high-purity and the antimony-doped samples are shown in Fig. 8. Within the exhaustion range and the intermediate temperature range, the resistivities as functions of temperature can be satisfactorily accounted for by the considerations set out in Sec. I. The experimental and the theoretical values of the mobilities for different samples are shown in Fig. 9. The experimental values of the mobilities are obtained from the relation

$$\mu = (1/r)(R/\rho), \quad (6)$$

where r is taken as $3\pi/8$.

The theoretical values of mobility are calculated from Eqs. (3), (4), and (5). Due to the simultaneous presence of donors and acceptors in a sample, the concentration of ionized impurity centers is not zero at zero absolute temperature, but is $N_0 = 2N_A$ in the case of N -type samples, or $N_0 = 2N_D$ in the case of P -type samples.⁹ The concentration of ionized impurity centers at any temperature is then given by

$$N_s = n + N_0. \quad (7)$$

N_0 is determined by fitting the theoretical mobility curve to the experimental points. The values of N_0 are listed in Table II.

The importance of N_0 in the mobility consideration is as follows: Since n decreases rapidly with temperature, without N_0 the mobility would increase rapidly

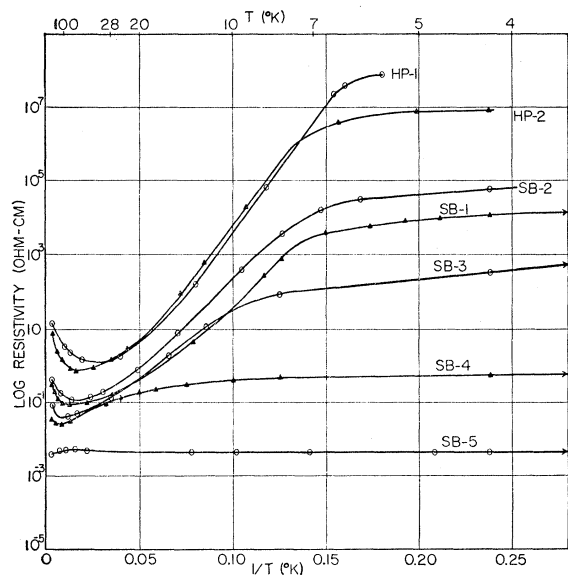


FIG. 8. Semilogarithmic plot of the resistivity vs reciprocal of Kelvin temperature for germanium samples HP-1, HP-2, SB-1, SB-2, SB-3, SB-4, and SB-5.

with decreasing temperature. Experimentally this is certainly not the case. The mobility passes through a maximum and then decreases slowly as the temperature is lowered.

For sample SB-5, the degeneracy temperature is around 100°K , and the theoretical mobility is calculated according to the considerations discussed by Johnson and Lark-Horovitz.⁴ Sample SB-2 is omitted from Fig. 8 to avoid confusion with the points of SB-1, since their mobilities are very close. The theoretical curve of SB-3 is absent because of the inhomogeneity of the sample.

Sample SB-4 has a high mobility in its donor band (see Sec. IV) so that only at relatively high temperatures could its mobility be analyzed in the above way. For sample SB-5 the concentration of impurity centers is so large that either the impurity band has completely overlapped with the conduction band or the mobilities

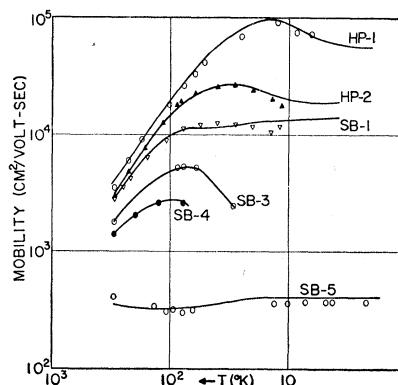


FIG. 9. Plot of log mobility vs log Kelvin temperature for germanium samples HP-1, HP-2, SB-1, SB-3, SB-4, and SB-5.

in the two bands are the same. The above analysis of the theoretical mobility applies in either case.

The resistivities of the neutron-bombarded samples are shown in Fig. 10. They have the same general shape as those of the high-purity and the antimony-doped samples. At liquid nitrogen temperature and above, the resistivity can be accounted for by lattice scattering plus impurity scattering, with $N_0 = 2N_D = n_0$, where n_0 is the number of holes in the exhaustion range.

In the low-temperature region the resistivities of all of the samples mentioned do not increase indefinitely as temperature is lowered but approach saturation values at temperatures corresponding to their respective Hall maxima.

IV. DISCUSSION

The results clearly indicate that the ordinary model, even if it is expanded to take into account the presence of both donor and acceptor levels, cannot explain the anomalous behavior of the Hall effect. This can only be understood if a mechanism is found which will introduce a combination of mobilities due to different types of scattering.

Schottky¹² has pointed out that, due to the random

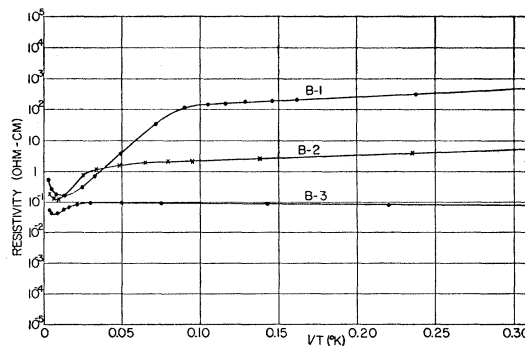


FIG. 10. Semilogarithmic plot of resistivity vs reciprocal of Kelvin temperature for neutron-bombarded germanium samples B-1, B-2, and B-3 (P -type).

¹² W. Schottky, Z. Elektrochem. 45, 33 (1939).

distribution of the impurity centers, the impurity states do not have one sharp energy level. Instead, the impurity levels form a band. This idea has been used by Busch¹³ in his discussion of the Hall effect in SiC. Lark-Horovitz and Johnson have considered this model to explain some of the anomalies in Hall curves. However, according to this picture of the impurity band, the impurity states remain localized states. Therefore, this picture cannot serve as a satisfactory basis for the explanation of our experimental results.

James and Ginzburg¹⁴ introduced the idea of an impurity band from a different point of view. According to them, the interaction between the impurity states, or the overlapping of their wave functions, causes the formation of an impurity band. The broadening of the impurity level into a band therefore means the "de-localization" of the impurity states. James pointed¹⁵ out the possibility of conduction in this impurity band.

The possibility of conduction in the impurity band as an explanation of the behavior of the Hall curves at low temperatures will now be presented:

(a) The Mobility of Electrons in the Donor States, or Holes in the Acceptor States

The impurity states are not strictly localized states as pictured in Fig. 1. Due to the finite distance between the impurity centers, an electron in one donor state has a finite probability of going over to another donor state in its spatial neighborhood provided that the latter is not occupied. When an electric field is applied, a small but finite conduction will take place in these impurity states.

It is assumed that the conductivity is proportional to the electric field applied; that is, a definite mobility may be assigned to these states. As the concentration of impurity centers is increased, the impurity states become less localized and the mobility increases accordingly. This mobility in the impurity states is usually small compared to the mobility of electrons in the conduction band or of holes in the filled band. At low temperatures, however, when the concentration of electrons in the conduction band becomes very small, the conduction in the donor states is no longer negligible. For samples of higher impurity concentration, the mobility of the impurity states is higher, and their effect will be felt at higher temperature.

(b) Picture of Simultaneous Conduction in the Conduction Band and in the Donor Impurity Band

The model of the impurity semiconductor as represented in Fig. 1 is now revised to that shown in Fig. 11.

¹³ G. Busch, *Helv. Phys. Acta* **19**, 189 (1946); G. Busch and H. Labhart, *Helv. Phys. Acta* **19**, 463 (1946).

¹⁴ A. S. Ginzburg, Ph.D. Thesis, Purdue University, 1949 (unpublished); Hubert M. James and Arthur S. Ginzburg, *J. Phys. Chem.* **57**, 840 (1953).

¹⁵ H. M. James (private communication); H. M. James and A. S. Ginzburg (reference 14).

The impurity states are now represented as narrow bands. The acceptor band is filled by electrons from the donor band and is inactive in conduction; n_c and n_D denote the concentration of electrons in the conduction band and in the donor band respectively; μ_c and μ_D denote the respective mobilities. The total number of electrons is

$$n_0 = n_c + n_D = N_D - N_A. \quad (8)$$

Since N_A is never zero, n_0 is necessarily smaller than N_D , the concentration of donor states. The donor band is, therefore, never filled, and conduction is assured at all temperatures.

The conductivity and the Hall coefficient for the semiconductor are now given by the following expressions:

$$\sigma = n_c e \mu_c + n_D e \mu_D, \quad (9)$$

$$R = - \frac{r (n_c \mu_c^2 + n_D \mu_D^2)}{e (n_c \mu_c + n_D \mu_D)^2}. \quad (10)$$

Equation (10) is adapted from the usual expression for the Hall coefficient in the intrinsic range of semiconductors and is assumed to hold when the electrons in the donor band are considered.

(c) The Limiting Case of High Temperature

Since μ_D is usually much smaller than μ_c at relatively high temperatures, when n_c is not too small, the following conditions are fulfilled:

$$n_c e \mu_c \gg n_D e \mu_D,$$

and

$$n_c e \mu_c^2 \gg n_D e \mu_D^2.$$

Thus the approximate expressions for the conductivity and the Hall coefficient are as follows:

$$\sigma = n_c e \mu_c, \quad (11)$$

$$R = r / n_c e. \quad (12)$$

Equations (11) and (12) are just the same as Eqs. (1) and (2). They are valid in the exhaustion range and in the intermediate-temperature range. The analysis of σ and R given in Sec. III, therefore, remains valid.

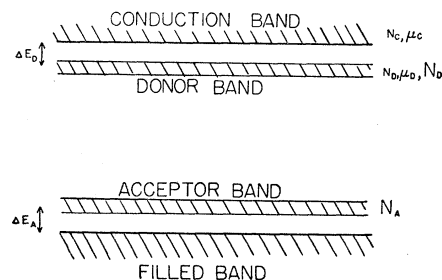


FIG. 11. Energy level diagram for an impurity semiconductor, modified to show finite width of donor and acceptor bands.

(d) The Limiting Case of Low Temperature

Because of the finite activation energy, ΔE_D , the electron concentration in the conduction band continues to drop as the temperature is lowered. Finally a temperature is reached at which

$$n_c \mu_c^2 \ll n_D e \mu_D^2, \quad n_c e \mu_c \ll n_D e \mu_D.$$

Then the σ and R expressions become

$$\sigma = n_D e \mu_D, \quad (13)$$

$$R = r/n_D e. \quad (14)$$

At low temperatures nearly all the electrons have fallen back to the donor states. Equation (14) then shows that the Hall coefficient is practically constant at very low temperatures, and that its value is just the same as the Hall coefficient in the exhaustion range when all the electrons are in the conduction band. This behavior is experimentally observed, approximately, for the low-resistance sample SB-4 and for the neutron-bombarded samples. The deviation of R at very low temperatures from its value at room temperature for these samples may come from the fact that the carriers in the impurity bands are not free carriers, and Eq. (10) is only approximately valid.

The ohmic behavior of the measured resistivity at low temperatures justified the previous assumption that definite mobility can be assigned to carriers in an impurity band. The flatness of the resistivity curves at very low temperatures indicates further that this mobility in an impurity band is approximately temperature-independent.

(e) The Intermediate Case

Since the Hall coefficients are the same at room (exhaustion) temperature and at extremely low temperature and since, also, the value of the Hall coefficient increases as the temperature is lowered below the exhaustion range, the Hall coefficient must pass through

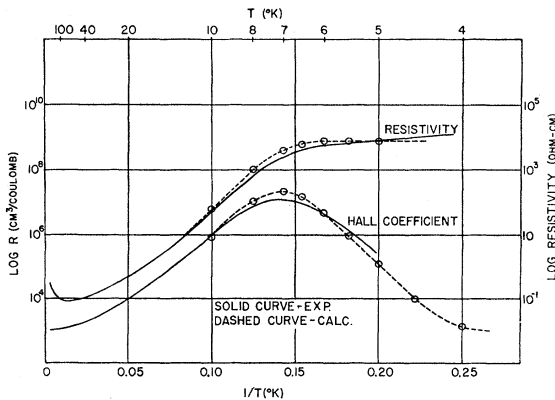


FIG. 12. Comparison of measured Hall and resistivity curves of antimony-doped germanium sample SB-1 (*N*-type) with the corresponding curves calculated on the basis of impurity band conduction.

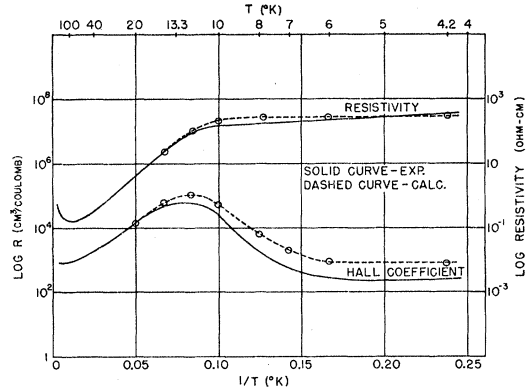


FIG. 13. Comparison of measured Hall and resistivity curves of neutron-bombarded germanium sample B-1 (*P*-type) with the corresponding curves calculated on the basis of impurity band conduction.

a maximum; this maximum in R explains the observed anomaly described in Sec. III.

The theoretical values of the Hall coefficient and the conductivity in the intermediate case can be obtained from Eqs. (9) and (10), provided that all the four quantities, n_c , n_D , μ_c , and μ_D , are known as functions of temperature.

In the case of a rather well defined energy gap ΔE_D , n_c is expected to decrease almost exponentially with $1/T$; then n_c , at low temperatures, can be obtained from a straight line extrapolation of the experimental $\ln(1/Re)$ vs $1/T$ curve.

n_D can be obtained from Eq. (8) and the information on n_c . It is practically a constant for temperatures corresponding to the intermediate case, except for the case of very low resistivity samples.

μ_c can be obtained by extending the mobility curves shown in Fig. 9 and with the help of Eqs. (3), (4), (5), and (7). As a first approximation, it can be considered as a constant.

μ_D is also practically constant with temperature as evidenced by the flatness of the resistivity curves shown in Figs. 8 and 10. Its value can be obtained from Eq. (13), in which σ is the measured value of conductivity at very low temperatures, and $n_D = n_0$.

The maximum in the Hall coefficient is found to occur when

$$n_c \mu_c = n_D \mu_D. \quad (15)$$

The calculated Hall coefficient and resistivity curves for samples SB-1 and B-1, together with the experimental points, are shown in Figs. 12 and 13. The agreement is seen to be satisfactory, considering the crude approximation in applying Eq. (10) to carriers in the impurity bands. The Hall coefficient and resistivity have also been calculated for the other samples and found to agree with experiment.

For the low-resistivity sample SB-5, which is *N*-type at all temperatures, the carriers in the donor band are definitely electrons. For the bombarded samples, which

are *P*-type at all temperatures studied, the carriers in the acceptor band are definitely holes. However, for the other higher resistivity samples, the sign of the carriers in the impurity bands cannot be easily ascertained. The difficulty lies in the fact that the resistivity at low temperatures and the Hall coefficient near the maximum of the Hall curve depend only on the absolute value of the product of n_D and μ_D , provided that μ_D is sufficiently smaller than μ_o .

(f) The Mobility of Carriers in the Impurity Bands versus the Concentration of Impurity Atoms

Values of mobilities for different samples as calculated from Eq. (13) are listed in Table II. If they are plotted as functions of the impurity concentration, there is considerable scattering in the points. Roughly, the curve can be represented by the relation

$$\mu_D = B(N_D)^\beta, \quad (16)$$

where β is close to 1.5. B seems to be somewhat different for the antimony-doped samples and for the neutron-bombarded samples.

The relation expressed by Eq. (16) is certainly very crude, since one would expect μ_D to depend not only on the concentration of impurity centers, but also on the type of impurity atoms introduced, and on how the impurity bands are filled. A definite picture of the mechanism of impurity bands has to be formed before one can predict the mobility and the sign of the carriers in these bands.

V. CONCLUSION

From the above discussion, it is seen that the behavior of the Hall and the resistivity curves over the

entire temperature range can be satisfactorily accounted for on the basis of simultaneous conduction by two kinds of carriers in different energy bands and with different mobilities. These two bands have been taken, in this discussion, as the conduction band and the donor band (or the filled and the acceptor band). It is important, however, to notice the difference between the impurity bands and the conduction and filled bands. First, the conduction and filled bands arise from the regular lattice structure, whereas the impurity bands arise from the randomly distributed impurity centers. The latter bands are therefore not homogeneous throughout the crystal. And, secondly, the impurity centers are usually so far apart that, although the impurity states are not strictly localized, the carriers in these states are far from being free. A theoretical investigation of the behavior of carriers in the impurity bands is very desirable. An experimental investigation of the mobility of carriers in the impurity bands as functions of the concentration of impurity centers and of the concentration of carriers, and also for different kinds of impurity centers, would be helpful to the theoretical study.

The authors wish to express their sincere gratitude to Dr. K. Lark-Horovitz for the suggestion of this work and his encouragement on which its success has depended. They are indebted to Dr. W. E. Taylor for the supply of the germanium samples, and to Professors H. Y. Fan, H. M. James, and V. A. Johnson for stimulating discussions. Lastly, their deepest gratitude is due Professor P. H. Keesom, whose advice, given throughout the course of this work, including the design of the cryostat, has been both generous and indispensable.